Rotordynamic Analysis of Textured Annular Seals With Multiphase (Bubbly) Flow[§]

Mihai ARGHIR*,[1], Abdelmalik ZERARKA[1], Gérard PINEAU[1]

*Corresponding author
*,[1] Institut Pprime, Université de Poitiers, ENSMA, UPR CNRS 3346
SP2MI, 11 Bd. Pierre et Marie Curie, BP 30179
86962 Futuroscope Chasseneuil Cedex, France.
mihai.arghir@univ-poitiers.fr

DOI: 10.13111/2066-8201.2011.3.3.1

Abstract: *For some applications it must be considered that the flow in the annular seal contains a mixture of liquid and gas. The multiphase character of the flow is described by the volume fraction of gas (usually air) contained in the liquid under the form of bubbles.*
The fluid is then a homogenous mixture of air and liquid all thru the annular seal. Its local gas volume fraction depends on the pressure field and is calculated by using a simplified form of the Rayleigh-Plesset equation.
The influence of such of a multiphase (bubbly) flow on the dynamic characteristics of a straight annular seal is minimal because the volume of the fluid is reduced.
The situation is quite different for textured annular (damper) seals provided with equally spaced deep cavities intended to increase the damping capabilities and to reduce the leakage flow rate.
As a by-product, the volume of the fluid in the seal increases drastically and the compressibility effects stemming from the bubbly nature of the flow are largely increased even for a low gas volume fraction. The present work depicts the influence of the gas volume fraction on the dynamic characteristics of a textured annular seal. It is shown that variations of the gas volume fraction between 1% and 0.1% can lead to frequency dependent stiffness, damping and added mass coefficients.

Key Words*: mixture of liquid, multiphase flow, textured annular seals, compressibility effects, damping capabilities.*

1. INTRODUCTION

Annular seals are used in high speed rotating machines (as for example turbopumps [1]) for minimizing the leakage between a high pressure zone from a low pressure one (Figure 1).

In order to avoid the contact between the vibrating rotor and the casing, the radial clearance is generally one order of magnitude larger than the one encountered in journal bearings.

Nevertheless, due to high rotation speeds and large pressure differences, the forces engendered in annular seals are of the same importance as in journal bearings and have the same impact on rotordynamics.

It is then of capital importance to accurately predict these forces.

[§] Publication presented at the Workshop "Dynamic Sealing Under Severe Working Conditions" EDF-LMS Futuroscope, October 5, 2009.

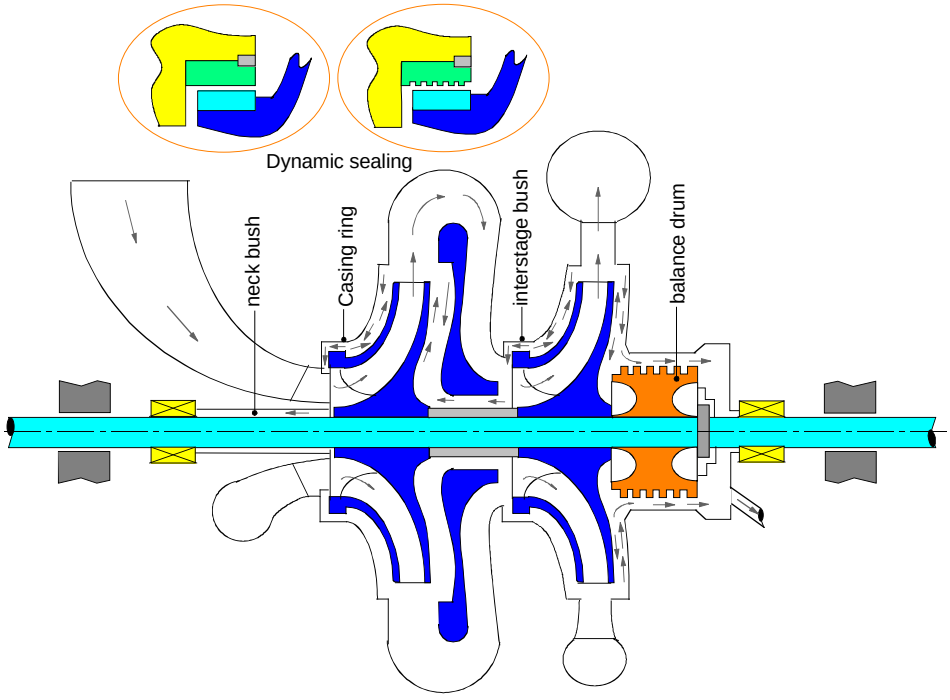

Figure 1. Annular seals in a centrifugal pump

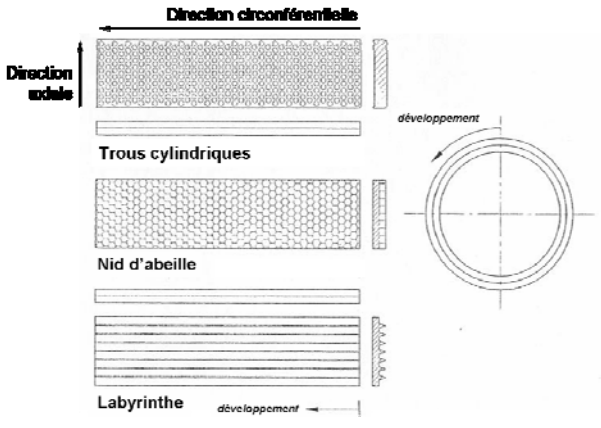

Figure 2. Stator texture in an annular seal [3]

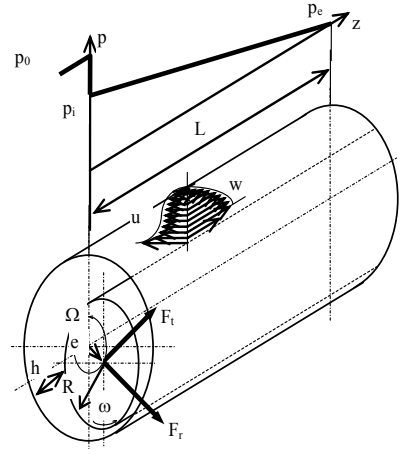

Figure 3. Pressure variation and velocities inside an annular seal

Annular seals usually work under high Reynolds numbers where convective inertia is dominant compared to viscous forces. The bulk-flow model is an appropriate model and represents a good compromise between accuracy and computational effort. Many aspects can be taken into account (turbulent and non-isothermal flow, compressible fluid) the most important being the dynamic regime. For some applications it must also be considered that the flow in the seal contains a mixture of liquid and gas but the literature tackling this latter aspect is peculiarly scarce. A recent theoretical work [2] tackles this subject having in view compressor stability problems encountered in the oil extraction industry. Clear experimental data on this subject are not available and efforts for adapting existing annular seals test rigs for multiphase flow are actually ongoing.

The multiphase character of the flow is described by the volume fraction of gas (usually air) contained in the liquid under the form of bubbles. This is not just a flow regime characterised by a low to mild compressibility and its description needs some supplementary assumptions. It is supposed that the gas is contained in spherical bubbles travelling with the velocity of the surrounding fluid (no slip between the liquid and the gas phase). The fluid is then a homogenous mixture of air and liquid all thru the annular seal. Its local gas volume fraction depends on the pressure field and is calculated by using a simplified form of the Rayleigh-Plesset equation. The influence of such of a multiphase (bubbly) flow on the dynamic characteristics of a straight annular seal is minimal because the volume of the fluid is reduced. The situation is quite different for textured annular (damper) seals. As depicted in Figure 2, the stator of these seals is provided with equally spaced deep cavities of cylindrical, knurled or honeycomb shape.

These cavities are intended to increase the damping capabilities and to reduce the leakage flow rate of the seal. As a by-product, the volume of the fluid in the seal increases drastically: the depth of these cavities is generally one order of magnitude larger than the seal clearance and they cover 30 to 70 % of the seal surface. As a consequence the compressibility effects stemming from the bubbly nature of the flow are largely increased even for a low gas volume fraction.

The present work depicts the influence of the gas volume fraction on the dynamic characteristics of a textured annular seal. It is shown that variations of the gas volume fraction between 10% and 0.1% can lead to the stiffness, damping and added mass coefficients depending on the excitation frequency.

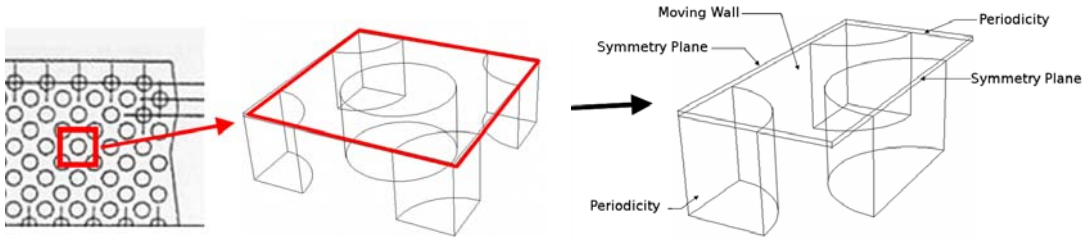

Figure 4. Texture cell used in Navier-Stokes calculations [4]

2. THE BULK FLOW MODEL AND ITS ADAPTATION FOR TEXTURED ANNULAR SEALS

The pressure variation and the velocities inside an annular seal are depicted in Figure 3. The thin film flow has mainly two components (axial and circumferential), the radial velocity being three order of magnitudes smaller.

The bulk flow model is based on Hirs assumption stating that the wall shear stresses in a thin film don't depend on the velocity profile or on the flow regime but only on the local Reynolds number.

$$\frac{\partial(\rho H)}{\partial t}+\rho\frac{\partial(HU)}{\partial x}+\rho\frac{\partial(HW)}{\partial z}=0 \tag{1}$$

$$\frac{\partial(\rho HU)}{\partial t}+\rho\frac{\partial(HUU)}{\partial x}+\rho\frac{\partial(HWU)}{\partial z}=-H\frac{\partial P}{\partial x}+\tau_{Rx}-\tau_{Sx} \tag{2}$$

$$\frac{\partial(\rho HW)}{\partial t}+\rho\frac{\partial(HUW)}{\partial x}+\rho\frac{\partial(HWW)}{\partial z}=-H\frac{\partial P}{\partial z}+\tau_{Rz}-\tau_{Sz} \tag{3}$$

Excepting the convective inertia effects, the bulk flow equations were obtained under the same simplifying assumptions as the more popular Reynolds equation used in Lubrication theory. It is to be noted that, as a by-product of Hirs assumptions, the viscous terms don't contain any derivatives and appear only as algebraic terms.

Only the convection terms contain derivatives. Therefore the bulk flow equations are valid only as long as the convection terms don't vanish, i.e. for $\mathrm{Re}^{*}=\mathrm{Re}\cdot C/R>1$ where Re^{*} describes the order of magnitude of convective forces compared to pressure and viscous effects. Following Hirs' assumption, the wall shear stresses depend only on the average (bulk) velocity and therefore can be estimated from the definition of the friction coefficient:

$$\tau_{R,S}=\rho V_{R,S}^{2}/2\cdot f_{S,R},\ V_S=\sqrt{W^2+U^2}\ \text{ and }\ V_R=\sqrt{W^2+(U-R\Omega)^2} \tag{4}$$

where V_S and V_R, are the stator and rotor relative velocities. The friction coefficients can be estimated by using any pipe friction law (Blasiu, Moody, etc.).

The bulk flow model was further adapted for taking into account the stator texture [4]. It was assumed that the textured annular sealed behaved as a straight annular seal of the same film thickness but with different stator and rotor friction laws. These laws were deduced from the results of complete Navier-Stokes calculations performed on elementary texture cells with periodic boundary conditions. Figure 4 depicts a detail of the texture extracted from the round holed pattern depicted in Figure 2. The stator and rotor friction laws were deduced by separately averaging the results of Navier-Stokes calculations over the stator surface S_3 and over the rotor (equivalent) surface $S_4 + S_5 + S_6$ as depicted in Figure 5. One then obtains an equivalent channel where the friction coefficients for the stator and the rotor are different but they both take into account the presence of the cell texture. These friction coefficients are cast under the usual form of a Blasius type law,

$$f_{R,S}^{i}=a_i\,\mathrm{Re}_i^{b_i}\ \text{ avec }\ \mathrm{Re}_i=2\rho CV_i/\mu \tag{5}$$

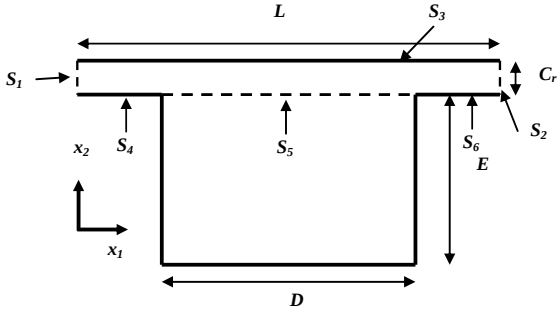

Figure 5. The texture cell and the equivalent channel (in red)

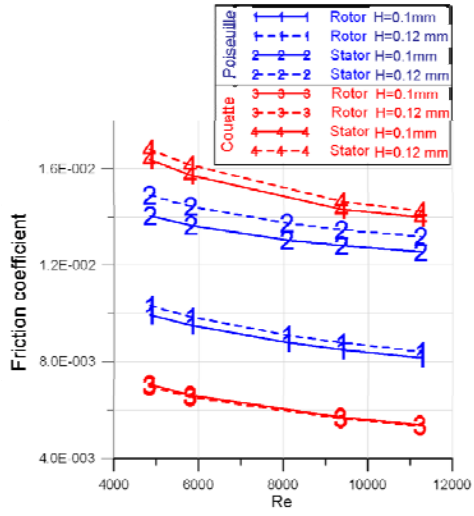

Figure 6. NS calculated friction coefficient [4]

It is to be underlined that coefficients *a* and *b* have different values for Poiseuille and Couette flow and they are not constant but depend on the film thickness. Reference [4] showed that they could be both approximated by $a = a_0 + a_1 C_r / L$ and $b = b_0 + b_1 C_r / L$ where $a_{0,1}$ and $b_{0,1}$ are constants. A problem still remains unanswered because, contrary to flows in a simple channel, the Poiseuille and the Couette friction laws are very different in a textured seal (Figure 6). For a straight annular seal, the Poiseuille and the Couette friction laws are not very different and thus enabled Hirs to formulate its model were only the film thickness averaged velocity is taken into account. The approach adopted in [4] for taking into account this result was to use the Poiseuille friction coefficients for the axial flow (that is driven by a pressure gradient between the inlet and outlet section of the annular seal) and the Couette friction coefficients for the circumferential flow that is mainly driven by the rotor viscous entrainment effect.

$$\tau_{Sz} = \frac{\rho V_S W}{2} f_S^{Poiseuille},\ \tau_{Sx} = \frac{\rho V_S U}{2} f_S^{Couette} \tag{6}$$

$$\tau_{Rz} = \frac{\rho V_R W}{2} f_R^{Poiseuille},\ \tau_{Rx} = \frac{\rho V_R (U - R\Omega)}{2} f_R^{Couette} \tag{7}$$

2.1. Further improvements of the textured annular seals "bulk flow" model

A further improvement of the model is to recognize that the volume of fluid contained in a textured annular seal is much larger that the one in a straight annular one. Indeed, the texture cells are one order of magnitude deeper than the radial clearance and they occupy 30…60% of the stator surface. The fact that a large volume of fluid is contained in the texture cell will permit under certain conditions a mass flow exchange with the seal main flow. For example if the rotor is eccentric, the thin film thickness $H = C - e_X \cos\theta - e_Y \sin\theta$ is not constant. A part of the cells of the texture lye on the convergent side while the other lye on the divergent part of the thin film. The flow can leave or enter the texture cell and the balance equations must then include some mass and impulse exchange between the thin film flow and the texture cell. This exchange is governed by the radial velocity at the stator surface, *V*. The bulk flow equations including this mass flow exchange between the texture and the main flow yield [5]:

$$\frac{\partial(\rho H)}{\partial t} + \rho \frac{\partial(HU)}{\partial x} + \rho \frac{\partial(HW)}{\partial z} + \rho V = 0 \tag{8}$$

$$\frac{\partial(\rho HU)}{\partial t} + \rho \frac{\partial(HUU)}{\partial x} + \rho \frac{\partial(HWU)}{\partial z} + \rho UV = -H \frac{\partial P}{\partial x} + \tau_{Rx} - \tau_{Sx} - T_x \tag{9}$$

$$\frac{\partial(\rho HW)}{\partial t} + \rho \frac{\partial(HUW)}{\partial x} + \rho \frac{\partial(HWW)}{\partial z} + \rho WV = -H \frac{\partial P}{\partial z} + \tau_{Rz} - \tau_{Sz} - T_z \tag{10}$$

The last terms on the left hand side of the bulk flow equations contain the mass and impulse exchange at the surface of the stator. It is obvious that for straight annular seals with a smooth stator $V = 0$. Estimating the radial velocity at the surface of the stator is not an easy task because the flow inside the texture cell is governed by viscous and inertia effects that escape to Lubrication simplifying assumptions. Nevertheless models using two or three additional control volumes for the flow inside the texture cell were proposed. These models

were first developed for grooved stator straight annular seals. For grooved stator straight annular seals, three control volume methods perform better than models based on two control volumes. Nevertheless, the textured annular seal contains a very large number of cells and it would be therefore very difficult to use such of model. The two control volume model remained then the only alternative and even this option has to be adapted for dealing with textured seals.

The main simplification is to consider the flow inside the texture cell as being governed only by the continuity equation.

$$\rho V = H_d \frac{\partial \rho}{\partial t} \tag{11}$$

where H_d is depth of the texture cell.

Following this equation the mass transfer between the texture and the thin film is possible only if the compressibility of the fluid is taken into account. Moreover, the radial velocity is non zero only for unsteady working conditions, $\partial/\partial t \neq 0$. For a liquid, the variation of its density is expressed by using the bulk modulus $B = \rho(\partial p/\partial \rho)_T$ and the radial velocity yields:

$$V = \frac{H_d}{B}\frac{\partial P}{\partial t} \tag{12}$$

where ρ and P are the density and the pressure inside the texture cell.

According to the thin film hypotheses, it is further assumed that the texture cell pressure is constant and is equal to the thin film pressure.

The compressibility of a liquid has very high values, for example for water or oil $B \approx 1.5 \ldots 2.3 \cdot 10^9\ Pa$.

This explains why the compressibility effects might be important only for very high excitation frequencies or very short time scales, $|\partial/\partial t| >> 1$. This is valid for a pure liquid. Oil, water and other liquid lubricants might contain non dissolved air bubbles that will modify the bulk modulus.

Following reference [6] the bulk modulus of a liquid lubricant containing a volume fraction α of non dissolved gas at pressure P is:

$$\frac{1}{B'} = \frac{1}{B} + \frac{\alpha}{P} \tag{13}$$

For example, if $B = 1.5 \cdot 10^9$ Pa and $P = 150$ bar then $B' = 90\%B$ for $\alpha = 0.1\%$ and $B' = 50\%B$ for $\alpha = 1\%$. The volume fraction of non dissolved gas can then modify the bulk modulus of the liquid lubricant.

Moreover, the bulk modulus depends on the local pressure not only because P is present in equation (13) but also because the gas volume fraction depends on it. The volume fraction of gas is defined as:

$$\alpha = \frac{\vartheta_g}{\vartheta} = \frac{\vartheta_g}{\vartheta_\ell + \vartheta_g} = \frac{\vartheta_g / \vartheta_\ell}{1 + \vartheta_g / \vartheta_\ell} = \frac{\overline{\vartheta}_g}{1 + \overline{\vartheta}_g},\ \overline{\vartheta}_g = \vartheta_g / \vartheta_\ell \tag{14}$$

The relative volume occupied by the non dissolved gas can be expressed by using the number of bubbles per unit liquid volume, η. It is supposed that all bubbles have the same radius, R_B. This yields:

$$\overline{\vartheta}_g = \eta \frac{4}{3}\pi R_B^3 \tag{15}$$

The gas volume fraction at a different pressure (for example at P_a = 1 bar) yields:

$$\alpha_a = \frac{\overline{\vartheta}_{g\,a}}{1+\overline{\vartheta}_{g\,a}},\ \overline{\vartheta}_{g\,a} = \eta_a \frac{4}{3}\pi R_{Ba}^3 \tag{16}$$

It is supposed that number of bubbles per unit liquid volume remains constant (the bubbles can change their size but the number remains the same), i.e. $\eta = \eta_a$. This yields:

$$\alpha = \frac{\alpha_a}{\alpha_a + \left(R_{Ba}/R_B\right)^3\left(1-\alpha_a\right)} \tag{17}$$

The gas volume fraction at pressure P can then be estimated if one knows α_a, R_{Ba} and $R_B(P)$. The variation of the bubble radius R_B with the local pressure is estimated from the Rayleigh Plesset equation.

2.2. The Rayleigh Plesset equation

It is supposed that the lubricant is a mixture of fluid and nuclei represented by spherical bubbles containing vapour and non dissolved gas. The RP equation describes the variation of the bubble radius at rest, surrounded by an infinite incompressible fluid and subject to an external pressure [7] :

$$\underbrace{p_B - p}_{(I)} - \underbrace{\frac{4\mu_L}{R}\frac{dR}{dt}}_{damping\ effect} - \underbrace{\frac{2S}{R}}_{surface\ tension} = \underbrace{\rho_L R\frac{d^2R}{dt^2} + \frac{3}{2}\rho_L\left(\frac{dR}{dt}\right)^2}_{inertia\ effects} \tag{18}$$

The first term *(I)* represents the difference between the pressure inside the bubble and the pressure in the surrounding fluid.

The simplified form of the RP used by Diaz's cavitation model [8] neglects the inertia terms, the damping terms and the surface tension effect. Actually, the RP equation is reduced to a simple equilibrium between the pressure inside and outside the bubble.

$$p_B - p = 0 \tag{19}$$

The bubble contains a mixture of non dissolved gas and fluid vapour. The bubble pressure can be expressed as the sum between the partial pressure of the non dissolved gas contained inside the bubble and the vapour pressure. This relation holds at pressure P as well at atmospheric conditions.

$$P_B = P_g + P_v,\ P_{Ba} = P_{ga} + P_v \tag{20}$$

The partial pressure of the non dissolved gas contained inside the bubble is expressed by using the state law of perfect gases and the assumption of an isothermal process from reference conditions, $P_g\ 4/3\,\pi R_B^3 = P_{ga}\ 4/3\,\pi R_{Ba}^3$. This yields:[**]

[**] The reference state is described by completely known feeding conditions, for example R_a and α_a for given p_a or for atmospheric pressure.

$$(P_B - P_v)R_B^3 = (P_{Ba} - P_v)R_{Ba}^3 = \left(\overbrace{p_a + 2S/R_{Ba}}^{P_{Ba}} - P_v\right)R_{Ba}^3 \tag{21}$$

By introducing the simplified form of the Rayleigh-Plesset equation (19) and by neglecting the vapour pressure and the surface tension effects one obtains:

$$P\frac{4}{3}\pi R_B^3 = P_a\frac{4}{3}\pi R_{Ba}^3 \tag{22}$$

The non dissolved gas volume fraction can then be calculated:

$$\alpha = \frac{\alpha_a}{\alpha_a + (P/P_a)(1-\alpha_a)} \tag{23}$$

The lubricant is considered as a homogeneous mixture of liquid and bubbles (the liquid and the gaseous phase have the same velocity) and its properties are calculated by using the volume fraction of gas [8]:

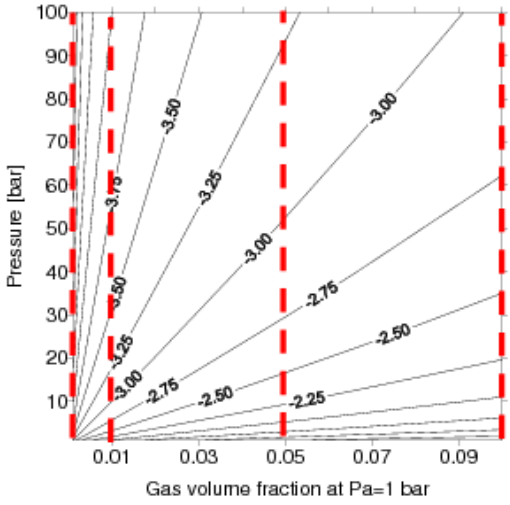

Figure 7. Logarithm of the gas volume fraction

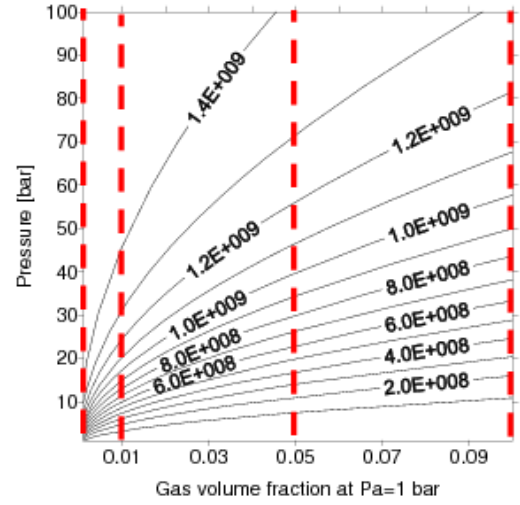

Figure 8. Bulk modulus of the liquid-air mixture

$$\rho = (1-\alpha)\rho_L + \alpha\rho_G \approx (1-\alpha)\rho_L,\ \ \mu = (1-\alpha)\mu_L + \alpha\mu_G \approx (1-\alpha)\mu_L \tag{24}$$

Figure 7 depict the gas volume fraction given by relation (23) for P/P_a comprised between 1 bar and 100 bar, typical for annular seals and for α_a comprised between 0.1% and 10%. The results show that large values of the ratio P/P_a compress the bubbles of non dissolved gas leading to values of α of the order of $10^{-2}\ldots10^{-3}$ or lower.

Therefore, for typical annular seals pressures, the contribution of the gas volume fraction on the density and viscosity can be neglected and relations (24) can be replaced by $\rho \approx \rho_L$ and $\mu \approx \mu_L$. Nevertheless, as depicted by Figure 8, the influence of the gas volume fraction on the bulk modulus given by equation (13) is not negligible. The same values of P/P_a and α_a show that when bubbles of non dissolved gas are present, the bulk modulus can be even one order of magnitude lower.

3. BULK FLOW ANALYSIS OF TEXTURED ANNULAR SEALS WITH BUBBLY FLOW

By injecting the radial velocity given by (12) in the bulk flow equations (8-10) one obtains:

$$\frac{\partial(\rho H)}{\partial t}+\rho\frac{\partial(HU)}{\partial x}+\rho\frac{\partial(HW)}{\partial z}+\left(H+H'_d\right)\frac{\rho}{B'}\frac{\partial P}{\partial t}=0 \tag{25}$$

$$\frac{\partial(\rho HU)}{\partial t}+\rho\frac{\partial(HUU)}{\partial x}+\rho\frac{\partial(HWU)}{\partial z}+\left(H+H'_d\right)\frac{\rho}{B'}\frac{\partial P}{\partial t}U=-H\frac{\partial P}{\partial x}+\tau_{Rx}-\tau_{Sx}-T_x \tag{26}$$

$$\frac{\partial(\rho HW)}{\partial t}+\rho\frac{\partial(HUW)}{\partial x}+\rho\frac{\partial(HWW)}{\partial z}+\left(H+H'_d\right)\frac{\rho}{B'}\frac{\partial P}{\partial t}W=-H\frac{\partial P}{\partial z}+\tau_{Rz}-\tau_{Sz}-T_z \tag{27}$$

The bulk modulus is calculated with equation (13) for taking into account the presence of non dissolved gas.

The texture depth was modified in a very approximate manner for taking into account that the texture covers only a part of the stator:

$$H'_d=\frac{S_{texture}}{S_{totale}}H_d \tag{28}$$

where $S_{totale}=\pi LD$ is the surface of the unwrapped annular seal and $S_{texture}$ is the surface occupied only by the texture.[††]

A centered annular seal taken from [4] and [9] with *L=35* mm, *D=76.5* mm, *C=100* μm working at Ω = 15500 rpm, P_{inlet} = 57 bar, P_{exit} = 1 bar and a circumferential velocity in the inlet section of *0.25RΩ* is analysed in the following. The seal is working with water so $\mu\approx\mu_\ell$ = *0.001* Pa·s and $\rho\approx\rho_\ell=10^3$ kg/m^3.

The stator is provided with a round hole pattern texture of depth H_d = *2* mm and diameter D_d = *3.175* mm covering 44 % of its surface.

As shown by equations (25-27) the bubbly character of the lubricant has an influence only for dynamic working conditions, i.e. $\partial/\partial t\neq 0$ therefore only the dynamic coefficients will be analysed. Figure 9 depicts the dynamic coefficients calculated for α_a = 0.1%, 1%, 5% and 10 % at P_a = 1 bar and different excitation speeds.

The four values of α_a are indicated with red lines in Fig. 7 and 8 showing that in all cases the gas volume fraction in the seal would be much lower that at atmospheric conditions. Indeed, the pressure inside the annular seal will be comprised between the inlet and the exit values (57 bar and 1 bar) so compression will decrease α.

Nevertheless, the bulk modulus B' is lower than the reference value used for a pure liquid, B=1.5·10^9 Pa.

For α_a = 0.1 % the influence of the gas volume fraction on the bulk modulus is negligible, $B'\approx B$, but for $\alpha_a\geq$ 5% the value of the bulk modulus is half or an order of magnitude lower than the reference value, $B'\approx(0.1...0.5)B$.

The dynamic compressibility of the fluid described by the bulk modulus will make the dynamic coefficients depend on the excitation frequency (for a pure liquid annular seal the dynamic coefficients don't depend on the excitation frequency).

[††] The total volume of fluid inside the annular seal is $HS_{totale}+H_dS_{texture}$.

The excitation frequencies used in Fig. 9 are comprised between *0.5Ω* and *4Ω*. One can see that modifications of the dynamic coefficients can be expected only for excitation frequencies higher than 2…3Ω.

The direct and the cross coupling stiffness coefficients increase very slightly for $\alpha_a \leq 1$ % and have a clear decrease for $\alpha_a \geq 5$ %.

The direct damping increases with the excitation frequency while the cross coupling damping and the direct added mass decrease with the excitation frequency.

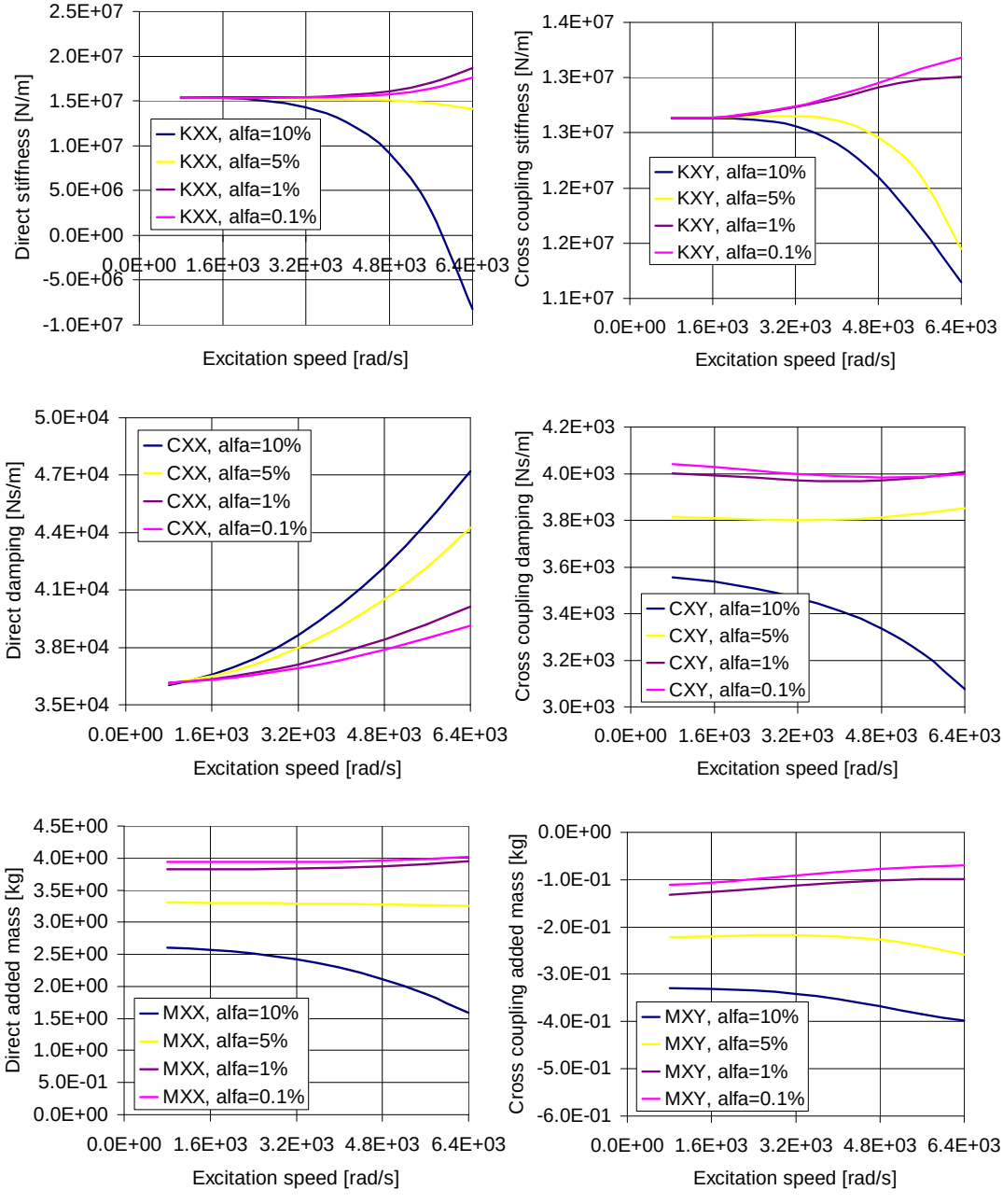

Figure 9. Rotordynamic coefficients versus the excitation speed

As depicted by Fig. 9, if $\alpha_a \leq 1$ % the gas volume fraction doesn't seem to have any influence and the variation of the dynamic coefficients with the excitation frequency seems to be only due to the reference bulk modulus of the pure liquid.

For $\alpha_a \geq 5$ % the situation is different and the influence of the volume fraction of non dissolved gas has a clear influence because the variation of stiffness coefficients is qualitatively different. These conclusions are quantitatively valid only for the textured annular seal used in the present analysis. For a different seal the influence of the compressibility of the liquid due to non dissolved gas will depend on the size and density of the texture cell.

4. CONCLUSIONS

The presence of a small volume fraction of non dissolved gas in the liquid can modify the dynamic coefficients of textured annular seals by rendering them dependent on the excitation frequency. The main modification are a diminution of the direct and cross coupling stiffness, of the cross coupling damping and of the direct added mass and an increase of the direct damping. The amount of these modifications depends on the volume fraction of non dissolved gas (for $\alpha_a \leq 1$ % all coefficients are frequency independent excepting the direct damping) and on the volume of the fluid contained inside the texture cell (this volume depends on the size and depth of the cell and on the texture density). Even if these modifications are not severe they should be considered when high excitation frequencies are present.

REFERENCES

[1] D. W. Childs, *Turbomachinery Rotordynamics. Phenomena, Modeling and Analysis*, John Wiley and Sons, 1993.

[2] L. San Andrés, Rotorydnamic Force Coefficients Of Bubbly Mixture Annular Pressure Seals, GT2011-45264.

[3] C. G. Holt and D. W. Childs, Theory Versus Experiment for the Rotordynamic Impedances of Two Hole-Pattern-Stator Gas Annular Seal, *ASME J. Trib*., **124** (1), pp. 137-143, 2002.

[4] F. Billy, *Analyse de f'effet des surfaces texturées dans un film mince. Application aux joints d'étanchéité (in French)*, Thèse de Docteur de l'Université de Poitiers, France, 2005.

[5] G. F. Kleynhans, D. W. Childs, The Acoustic Influence of Cell Depth on the Rotordynamic Characteristics of Smooth-Rotor/Honeycomb-Stator Annular Gas Seals, *ASME J. of Engineering for Gas Turbines and Power,* **119** (4), pp. 949-957 (96-GT-122), 1997.

[6] M. Guillon, *Commande et asservissement hydrauliques et électrohydrauliques*, Techniques et Documentation, Lavoisier, 1992.

[7] C. E. Brennen, *Cavitation and bubble dynamics*, Oxford Engineering Series 44, Oxford University Press, New York, 1995.

[8] S. E. Diaz, *The effect of air entrapment on the performance of squeeze film dampers: experiments and analysis*, Ph.D. dissertation, Texas A&M University, College Station, TX, 1999.

[9] D. W. Childs and P. Fayolle, Test Results for Liquid "Damper" Seals Using a Round-Hole Roughness Pattern for the Stators, *ASME J. Tribol.*, **121** (1), pp. 42-49, 1999.